Reducing Streaking Artifacts in Quantitative Susceptibility Mapping

Palacios, Benjamin

2017

Palacios , B , Uhlmann , G & Wang , Y 2017 , ' Reducing Streaking Artifacts in Quantitative Susceptibility Mapping ' , SIAM journal on imaging sciences , vol. 10 , no. 4 , pp. 1921-1934 . https://doi.org/10.1137/

http://hdl.handle.net/10138/313121
https://doi.org/10.1137/16M1096475

acceptedVersion

REDUCING STREAKING ARTIFACTS IN QUANTITATIVE SUSCEPTIBILITY MAPPING

BENJAMIN PALACIOS, GUNTHER UHLMANN, AND YIRAN WANG

Abstract. It is well-known that reconstruction algorithms in quantitative susceptibility mapping often contain streaking artifacts. In [1], the cause of the artifacts is identified as propagation of singularities. In this work, we analyze such singularities carefully and propose some strategies to reduce the artifacts.

1. The inverse problem

The goal of quantitative susceptibility mapping (QSM) is to provide images of the magnetic susceptibility distribution χ inside the human body. We refer to [17, 18] for the detailed background. Roughly speaking, when a tissue is put in a known magnetic field $\mathbf{H}$, it acquires a magnetic moment $\mathbf{M}$. The magnetic susceptibility χ of the tissue is defined by $\mathbf{M} = \chi\mathbf{H}$ where χ represents the electronic perturbation in the tissue. QSM aims to reconstruct χ from the measured local field perturbations. Actually, the experiment is carried out in a magnetic resonance (MR) scanner. The tissue is put in a known magnetic field and we measure the field ψ associated with the magnetization polarized by the main magnetic field of the MR scanner. Mathematically, this process can be described by

$$\psi(x) = \text{p.v.} \int_{\mathbb{R}^3} d(x - x')\chi(x')dx', \tag{1.1}$$

where $x = (x_1, x_2, x_3), x' = (x_1', x_2', x_3') \in \mathbb{R}^3$ and p.v. denotes the principal value of the singular integral with kernel

$$d(x) = \frac{2x_3^2 - x_1^2 - x_2^2}{4\pi|x|^5}, \quad x \in \mathbb{R}^3.$$

The inverse problem is to find χ given ψ, which is a deconvolution problem.

It is convenient to work in the Fourier domain. Denote the Fourier transform of f by $\hat{f}$. By taking the Fourier transform of (1.1), we obtain that

$$\hat{\psi}(\xi) = D(\xi)\hat{\chi}(\xi), \quad \xi = (\xi_1, \xi_2, \xi_3) \in \mathbb{R}^3, \tag{1.2}$$

where

$$D(\xi) = \frac{1}{3} - \frac{\xi_3^2}{|\xi|^2}.$$

The inverse problem of QSM is equivalent to recover $\hat{\chi}$ from $\hat{\psi}$. It is clear that the problem is ill-posed due to the presence of zeros of $D(\xi)$. In practice, since the data ψ may contain errors, it is noticed that the reconstructed image of χ is often contaminated by streaking artifacts, see [1] and the references therein. For example, see Figure 1. There have been several works on removing the artifacts, mostly based on regularization techniques, see [17, 18] for a review and references. In [1], the authors performed the mathematical study of QSM. For ψ in a suitable distribution space, the existence, uniqueness and reconstruction formulas are obtained in [1, Theorem 2.2]. Also, the cause

of the streaking artifacts are identified as propagation of singularities for wave-type operators. In this note, we analyze the streaking artifacts in more detail. We will give a more precise description of the singularities under some assumptions and propose some strategies to reduce the streaking artifacts. The microlocal analysis of the singularities involves paired Lagrangian distributions that were introduced in [16] and further studied on [3, 4, 5, 6, 7, 8, 9]. In particular, the method developed in this paper could be applied to reduce artifacts for restricted X-ray transforms [6, 4] like the X-ray transform with sources on a curve.

2. Streaking artifacts and propagation of singularities

As discussed in [1, Section 2.2], equation (1.2) is equivalent to the wave equation on $\mathbb{R}^2$. Actually, multiplying (1.2) by $|\xi|^2$ and taking the inverse Fourier transform, we obtain that

$$P(\partial)\chi(x) = -\Delta\psi(x), \tag{2.1}$$

where $P(\partial)$ is the wave-type operator

$$P(\partial) = \frac{2}{3}\frac{\partial^2}{\partial x_3^2} - \frac{1}{3}(\frac{\partial^2}{\partial x_1^2} + \frac{\partial^2}{\partial x_2^2}), \tag{2.2}$$

and $\Delta = \sum_{i=1}^3 \frac{\partial^2}{\partial x_i^2}$ is the Laplacian on $\mathbb{R}^3$. It is well-known that the wave operator $P(\partial)$ has a fundamental solution i.e. there exits $Q \in \mathcal{D}'(\mathbb{R}^3 \times \mathbb{R}^3)$, the space of distributions on $\mathbb{R}^3 \times \mathbb{R}^3$, such that

$$P(\partial)Q = \delta,$$

where δ is the delta distribution on $\mathbb{R}^3$. In fact, one can write down an expression of Q explicitly i.e. $Q(x, x') = g(x - x')$ where

$$g(x) = \begin{cases} \dfrac{3}{4\pi\sqrt{x_3^2 - 2(x_1^2 + x_2^2)}}, \text{ for } 2(x_1^2 + x_2^2) < x_3^2, \\ 0, \text{ otherwise} \end{cases} \tag{2.3}$$

see (3.2) in [1]. Q defines a continuous linear map from $C_0^\infty(\mathbb{R}^3)$ to $\mathcal{D}'(\mathbb{R}^3)$ (by e.g. Schwartz kernel theorem). Hereafter we do not distinguish the notation for the operator and its Schwartz kernel. For $\psi \in C_0^\infty(\mathbb{R}^3)$, we can express the solution χ to (2.1) simply as

$$\chi = Q(-\Delta\psi) = -g * (\Delta\psi), \tag{2.4}$$

which is a convolution. The extension of Q to distributions was done in [1]. Here we give an exposition using microlocal techniques. Also, we give a detailed description of the singularities of χ.

It is easy to see that the singular support of Q is the set $\{x \in \mathbb{R}^3 : 2(x_1^2 + x_2^2) = x_3^2\}$. Recall that for any distribution ϕ, the singular support of ϕ, denoted by singsupp(ϕ), is defined as the closure of the complement of the set where ϕ is smooth. To get a more precise description of the singularities, we use the notion of wave front sets (see for example [2, 10]) defined on the cotangent space $T^*\mathbb{R}^3$ which can be identified with the product space $\mathbb{R}^3 \times \mathbb{R}^3$. For $\phi \in \mathcal{D}'(\mathbb{R}^3)$, the wave front set WF($\phi$) is a conic set in $T^*\mathbb{R}^3\backslash 0$ and by definition, $(x', \xi') \notin \text{WF}(\phi)$ if there exists a conic neighborhood $\Gamma \subset T^*\mathbb{R}^3\backslash 0$ of (x', ξ') such that for any $N > 0$, there is $C_N > 0$ such that

$$|\hat{\phi}(\xi)| \leq C_N|\xi|^{-N}, \quad (x, \xi) \in \Gamma.$$

It is a fact that $\pi(\text{WF}(\phi)) = \text{singsupp}(\phi)$ where $\pi : T^*\mathbb{R}^3 \to \mathbb{R}^3$ denotes the natural projection $\pi(x, \xi) = x$.

The fundamental solution Q belongs to a special class of distributions, namely the paired Lagrangian distributions. In particular, the wave front set of Q consists of two intersecting Lagrangian submanifolds. The theory for such distributions is developed in [3, 16, 9, 6, 7]. It is now widely used in microlocal analysis and inverse problems, see for example [4, 5, 13, 14, 15].

We describe the two Lagrangians first. Let $\xi = (\xi_1, \xi_2, \xi_3) \in T^*_x\mathbb{R}^3$ be the dual variables to $x = (x_1, x_2, x_3) \in \mathbb{R}^3$. It is well-known that $T^*\mathbb{R}^3$ is a symplectic manifold with canonical two form given by

$$\omega = d\xi \wedge dx = \sum_{i=1}^{3} d\xi_i \wedge dx_i.$$

A submanifold $\Lambda \subset T^*\mathbb{R}^3$ is called Lagrangian if $\dim \Lambda = 3$ and the canonical two form ω vanishes on Λ. A Lagrangian manifold Λ is conic if $(x, \lambda\xi) \in \Lambda$ for any $(x, \xi) \in \Lambda$ and $\lambda > 0$. Let $p(\xi)$ be the symbol of $P(\partial)$ i.e. $p(\xi) = -\xi_3^2 + \frac{1}{3}|\xi|^2$. The characteristic set of p is $\Sigma = \{(x, \xi) \in T^*\mathbb{R}^3 : p(\xi) = 0\}$. We denote the Hamilton vector field of p by H_p. Explicitly, we have

$$H_p = \sum_{i=1}^{3} (\frac{\partial p}{\partial \xi_i}\frac{\partial}{\partial x_i} - \frac{\partial p}{\partial x_i}\frac{\partial}{\partial \xi_i}) = \frac{2}{3}(\xi_1\frac{\partial}{\partial x_1} + \xi_2\frac{\partial}{\partial x_2}) - \frac{4}{3}\xi_3\frac{\partial}{\partial x_3}.$$

Notice that H_p is tangent to Σ. The integral curves of H_p in Σ are called null bicharacteristics. It is a well-known fact that the projections of null bicharacteristics to the base manifold are geodesics. In our case, the base manifold is $\mathbb{R}^3$ with Lorentzian metric $g = -\frac{3}{2}dx_3^2 + 3(dx_1^2 + dx_2^2)$ so the geodesics are straight lines. More precisely, for any $(x', \xi') \in \Sigma$, we denote the null bicharacteristics by $\gamma_{x',\xi'}(s), s \in \mathbb{R}$. Then we find that

$$\gamma_{x',\xi'}(s) = (x' + sdp(\xi'), \xi'),$$

where $dp(\xi) = (\frac{2}{3}\xi_1, \frac{2}{3}\xi_2, -\frac{4}{3}\xi_3)$. The projection of $\gamma_{x',\xi'}$ to $\mathbb{R}^3$ is just $x' + sdp(\xi')$ which is a straight line.

We also work on the product space $\mathbb{R}^3 \times \mathbb{R}^3$ since Q is a distribution defined there. We can regard the symbol p as a function on $T^*\mathbb{R}^3 \times T^*\mathbb{R}^3$ by lifting it from the left factor i.e. $p(\xi, \xi') = p(\xi)$. Similarly, we identify Σ, H_p as objects on $T^*\mathbb{R}^3 \times T^*\mathbb{R}^3$. We let

$$\text{Diag} = \{(x, x') \in \mathbb{R}^3 \times \mathbb{R}^3 : x = x'\}$$

be the diagonal of the product space and

$$N^*\text{Diag} = \{(x, x'; \xi, \xi') \in T^*\mathbb{R}^3 \times T^*\mathbb{R}^3 : x = x', \xi' = -\xi, \xi \neq 0\}$$

be the conormal bundle of Diag. This is a conic Lagrangian submanifold in $T^*(\mathbb{R}^3 \times \mathbb{R}^3)$ with canoic two form $\tilde{w} = d\xi \wedge dx + d\xi' \wedge dx'$, and gives the normal direction to Diag. Let Λ_p be the conic Lagrangian manifold in $T^*(\mathbb{R}^3 \times \mathbb{R}^3)$ obtained from flowing out $N^*\text{Diag} \cap \Sigma$ under H_p. Actually, this can be written down explicitly as

$$\Lambda_p = \{(x' + sdp(\xi'), \xi', x', -\xi') \in T^*\mathbb{R}^3\backslash 0 \times T^*\mathbb{R}^3\backslash 0 : x' \in \mathbb{R}^3, s \in \mathbb{R}, \quad p(\xi') = 0\}. \tag{2.5}$$

It is proved in [16] that the fundamental solution $Q \in I^{-\frac{3}{2},-\frac{1}{2}}(N^*\text{Diag}, \Lambda_p)$. We will explain this notion especially the meaning of the orders in the next section. For now, we just need the fact that the wave front set $\text{WF}(Q) \subset N^*\text{Diag} \cup \Lambda_p$.

Let's recall the wave front relation for $E \in \mathcal{D}'(\mathbb{R}^3 \times \mathbb{R}^3)$ which is

$$\text{WF}'(E) = \{((x, \xi), (x', \xi')) \in T^*\mathbb{R}^3 \times T^*\mathbb{R}^3\backslash 0 : (x, x'; \xi, -\xi') \in \text{WF}(E)\}.$$

For two wave front relations $R_1, R_2 \subset T^*\mathbb{R}^3 \times T^*\mathbb{R}^3$, the composition is defined as

$$R_1 \circ R_2 = \{((x,\xi),(x'',\xi'')) : \exists (x',\xi') \in T^*\mathbb{R}^3 \text{ s.t. } ((x,\xi),(x',\xi')) \in R_1, ((x',\xi'),(x'',\xi'')) \in R_2\}.$$

Now we have the following result on the solvability of QSM (compare with Theorem 3.3 of [1]).

Proposition 2.1. *Q can be extended to a sequentially continuous mapping: $\mathcal{E}'(\mathbb{R}^3) \to \mathcal{D}'(\mathbb{R}^3)$. For $\psi \in \mathcal{E}'(\mathbb{R}^3)$, there exists a solution $\chi = Q(-\Delta\psi) \in \mathcal{D}'(\mathbb{R}^3)$ to (2.1) and*

$$\mathrm{WF}(\chi) \subset \mathrm{WF}(\psi) \cup (\Lambda_p' \circ \mathrm{WF}(\psi)).$$

Moreover, for any $(x,\xi) \in (\mathrm{WF}(\chi) \setminus \mathrm{WF}(\psi)) \cap \Sigma$, let $\gamma_{x,\xi}$ be the bicharacteristics from (x,ξ). Then $\gamma_{x,\xi} \subset \mathrm{WF}(\chi)$.

Proof. The extension of Q to $\mathcal{E}'(\mathbb{R}^3)$ and the wave front relation are direct consequences of Corollary 1.3.8 of [2]. Here we used $\mathrm{WF}(\Delta\psi) = \mathrm{WF}(\psi)$ because Δ is an elliptic differential operator, see for example Corollary 8.3.2 of [10]. The last conclusion follows from the standard propagation of singularities result for wave operators (more generally operators with real principal part), see for example Theorem 8.3.3 of [11]. □

We remark that among the wave front set of Q, $N^*\mathrm{Diag}$ does not move the singularities of ψ, however, Λ_p does. We know a priori that χ is compactly supported hence $\mathrm{singsupp}(\chi)$ is compact. We easily obtain the following solvability result of the inverse problem (compare with Theorem 2.2 of [1]).

Proposition 2.2. *Suppose $\psi \in \mathcal{E}'(\mathbb{R}^3)$ and $\mathrm{WF}(\psi) \cap \Sigma = \emptyset$. Then there exists $\chi \in \mathcal{D}'(\mathbb{R}^3)$ to*

$$P(\partial)\chi = -\Delta\psi,$$

such that $\mathrm{singsupp}(\chi) \subset \mathrm{singsupp}(\psi)$ is compact.

The reconstruction formula of χ is obtained in Theorem 2.2 [1].

Based on the two propositions, the streaking artifacts can be identified as the set $\mathrm{WF}(\chi) \setminus \mathrm{WF}(\psi)$. This is because for any $(x,\xi) \in \mathrm{WF}(\chi) \setminus \mathrm{WF}(\psi)$, the whole bicharacteristics $\gamma_{x,\xi}$ is in $\mathrm{WF}(\chi)$ and this is not compactly supported. The projection of $\gamma_{x,\xi}$ to $\mathbb{R}^3$ is the straight line from x in ξ direction. This also agrees with the numerical results, see Figure 1 of [1]. Since the set $\mathrm{WF}(\chi) \setminus \mathrm{WF}(\psi)$ is contained in $(\Lambda_p' \circ \mathrm{WF}(\psi)) \setminus \mathrm{WF}(\psi)$, we shall regard the latter as the set of streaking artifacts in the following analysis.

3. Reduction of the streaking artifacts

For $\psi \in \mathcal{E}'(\mathbb{R}^3)$, we decompose the solution χ to (2.1) to separate the streaking artifacts. Since the streaking artifacts are caused by $\mathrm{WF}(\psi) \cap \Sigma$, we decompose ψ as following. Let $f \in C_0^\infty(\mathbb{R})$ be a cut-off function such that $f(t) = 1, |t| < 1$ and $f(t) = 0, |t| > 2$. Also, we let $g \in C_0^\infty(\mathbb{R}^3)$ be a cut-off function such that $\mathrm{supp}\ (\chi) \subset \mathrm{supp}\ (g)$. For $\epsilon > 0$, we define a pseudo-differential operator B_ϵ of order 0 associated with the (full) symbol

$$b_\epsilon(x,\xi) = g(x) f(p(\xi)/\epsilon). \tag{3.1}$$

Here we recall that a pseudo-differential operator A of order m is defined by an oscillatory integral

$$Au(x) = \frac{1}{(2\pi)^3} \int_{\mathbb{R}^3} e^{i(x-x')\xi} a(x,\xi) u(x') dx' d\xi, \quad a(x,\xi) \in S^m(\mathbb{R}^3 \times \mathbb{R}^3),$$

where $S^m(\mathbb{R}^3 \times \mathbb{R}^3)$ denotes the standard symbol class i.e. for $a \in S^m(\mathbb{R}^3 \times \mathbb{R}^3)$ and for any compact set K of U, we have

$$|\partial_x^\alpha \partial_\xi^\beta a(x,\xi)| \le C_{K,\alpha,\beta} \langle \xi \rangle^{m-|\beta|}, \quad C_{K,\alpha,\beta} > 0,$$

see e.g. [11, Section 18.1]. a is called the (full) symbol of A and the principal symbol is defined in $S^m(\mathbb{R}^3\times\mathbb{R}^3)/S^{m-1}(\mathbb{R}^3\times\mathbb{R}^3)$. We denote the space of pseudo-differential operators of order m by $\Psi^m(\mathbb{R}^3)$. Observe that in (3.1) b_ϵ vanishes for $p(\xi)>2\epsilon$ and $1-b_\epsilon$ vanishes for $p(\xi)<\epsilon$. Therefore, $\mathrm{WF}((\mathrm{Id}-B_\epsilon)\psi)\cap\Sigma=\emptyset$. We can write

$$\chi=\chi_1+\chi_2,\ \text{where } \chi_1=Q(\mathrm{Id}-B_\epsilon)(-\Delta\psi),\quad \chi_2=QB_\epsilon(-\Delta\psi). \tag{3.2}$$

By Proposition 2.1, we see that $\mathrm{WF}(\chi_1)\subset\mathrm{WF}(\psi)$ hence the streaking artifacts are contained in χ_2. One can remove the artifacts by simply taking χ_1 as the reconstruction. However, this would remove all the singularities of χ on $\mathrm{WF}(\psi)\cap\Sigma$ and this would result in a loss of information. See Figure 2.

To improve the results, in the following, we shall assume that the singularities of ψ have special structure i.e. the singularities are in the normal directions of some submanifolds. These are called conormal distributions and they appear often in applications. For example, the delta distribution δ. We see that $\mathrm{singsupp}(\delta)=\{0\in\mathbb{R}^3\}$ and $\mathrm{WF}(\delta)=T^*_0\mathbb{R}^3\backslash 0$. Here 0 represents the zero section of $T^*\mathbb{R}^3$. Another example is the characteristic function $\mathbf{1}_\Omega$ where Ω is a bounded domain with smooth boundary $\partial\Omega$. We have $\mathrm{singsupp}(\mathbf{1}_\Omega)=\partial\Omega$ and $\mathrm{WF}(\mathbf{1}_\Omega)=\{(x,\xi)\in T^*\mathbb{R}^3: x\in\partial\Omega,\langle\xi,\theta\rangle=0,\forall\theta\in T_x(\partial\Omega)\}$. The conormal bundle N^*K of a submanifold $K\subset\mathbb{R}^3$, defined as

$$N^*K=\{(x,\xi)\in T^*\mathbb{R}^3\backslash 0:\langle\xi,\theta\rangle=0,\theta\in T_xK\},$$

is a conic Lagrangian submanifold of $T^*\mathbb{R}^3\backslash 0$. In particular, $\mathrm{WF}(\delta)=N^*\{0\}$ and $\mathrm{WF}(\mathbf{1}_\Omega)=N^*(\partial\Omega)$.

We recall the basics of Lagrangian and paired Lagrangian distributions. The details can be found in for example [3, 11]. Let Λ be a smooth conic Lagrangian submanifold of $T^*\mathbb{R}^3\backslash 0$. Following the standard notation, we denote by $I^\mu(\Lambda)$ the space of Lagrangian distributions of order μ associated with Λ. In particular, for U open in $\mathbb{R}^3$, let $\phi(x,\xi):U\times\mathbb{R}^N\to\mathbb{R}$ be a smooth non-degenerate phase function (homogeneous of degree 1 in ξ) that locally parametrizes Λ i.e.

$$\{(x,d_x\phi)\in T^*_U\mathbb{R}^3\backslash 0: x\in U,\quad d_\xi\phi=0\}\subset\Lambda.$$

Then $u\in I^\mu(\Lambda)$ can be locally written as a finite sum of oscillatory integrals

$$\int_{\mathbb{R}^N}e^{i\phi(x,\xi)}a(x,\xi)d\xi,\quad a\in S^{\mu+\frac{3}{4}-\frac{N}{2}}(U\times\mathbb{R}^N).$$

For $u\in I^\mu(\Lambda)$, we know that $\mathrm{WF}(u)\subset\Lambda$. Also, for any $s<-\mu-\frac{3}{4}$, we have $u\in H^s(\mathbb{R}^3)$. So the order μ indicates the regularity of u. For a submanifold $Y\subset\mathbb{R}^3$, we denote $I^\mu(Y)=I^\mu(N^*Y)$ and these are called conormal distributions to Y.

For two Lagrangians $\Lambda_0,\Lambda_1\subset T^*X\backslash 0$ intersecting cleanly at a codimension k submanifold i.e.

$$T_x\Lambda_0\cap T_x\Lambda_1=T_x(\Lambda_0\cap\Lambda_1),\quad\forall x\in\Lambda_0\cap\Lambda_1,$$

the paired Lagrangian distribution associated with (Λ_0,Λ_1) is denoted by $I^{p,l}(\Lambda_0,\Lambda_1)$. Locally, paired Lagrangian distributions can be written as an oscillatory integral with a symbol of product type, see e.g. [3]. For $u\in I^{p,l}(\Lambda_0,\Lambda_1)$, we know that $\mathrm{WF}(u)\subset\Lambda_0\cup\Lambda_1$. In particular, microlocally away from the intersection $\Lambda_0\cap\Lambda_1$, we have that $u\in I^{p+l}(\Lambda_0\backslash\Lambda_1)$ and $u\in I^p(\Lambda_1\backslash\Lambda_0)$. For example, we know that the fundamental solution $Q\in I^{-\frac{3}{2},-\frac{1}{2}}(N^*\mathrm{Diag},\Lambda_p)$ so that $Q\in I^{-2}(N^*\mathrm{Diag}\backslash\Lambda_p)$ and $Q\in I^{-\frac{3}{2}}(\Lambda_p\backslash N^*\mathrm{Diag})$.

We need the following result to reduce the streaking artifacts.

Proposition 3.1. *Let Y be a submanifold of $\mathbb{R}^3$ with codimension ≥ 1 and assume that N^*Y intersect Σ transversally and each null bicharacterstics intersects N^*Y a finite number of times.*

Let Λ_Y denote the flow out of N^*Y under the Hamiltonian flow (2.5). Let $K \in I^{p,l}(N^*Diag, \Lambda_p)$ and $R \in \Psi^s(\mathbb{R}^3)$ properly supported. For $f \in I^\mu(Y) \cap \mathcal{E}'(\mathbb{R}^3)$, we have

1. *$Rf \in I^{s+\mu}(Y)$.*
2. *$K \circ Rf \in I^{p+s+\mu,l}(N^*Y, \Lambda_Y)$ so $K \circ Rf \in I^{p+s+\mu+l}(N^*Y \backslash \Lambda_Y) \cap I^{p+s+\mu}(\Lambda_Y \backslash N^*Y)$.*
3. *If the principal symbol of R vanishes on Λ_Y, we have*

$$R \circ Kf \in I^{p+\mu+l+s}(N^*Y \backslash \Lambda_Y) \cap I^{p+\mu+s-1}(\Lambda_Y \backslash N^*Y).$$

We make several remarks. First, one can think of the singularity on N^*Y as the true singularity in Kf and the one on Λ_Y as streaking artifacts. For $s < 0$, part (2) says that one can reduce the singularity on the two pieces simultaneously. For $s = 1$, part (3) tells one can increase the singularities on N^*Y while the one on Λ_Y stays the same. Second, if R is of order 1, the conclusion $R \circ Kf \in I^{p+\mu}(\Lambda_Y \backslash N^*Y)$ in part (3) just follows from the equivalent definition of Lagrangian distributions, see e.g. [12, Definition 25.1.1].

Proof of Prop. 3.1. (1) Let $k \geq 1$ be the codimension of Y. Locally we can choose local coordinate $x = (\bar{x}, \hat{x}), \bar{x} \in \mathbb{R}^{3-k}, \hat{x} \in \mathbb{R}^k$ such that $Y = \{\hat{x} = 0\}$. We let the dual variables $\xi = (\bar{\xi}, \hat{\xi}), \bar{\xi} \in \mathbb{R}^{3-k}, \hat{\xi} \in \mathbb{R}^k$. Then $N^*Y = \{\hat{x} = 0, \bar{\xi} = 0\}$. We can write $f \in I^\mu(Y)$ as an oscillatory integral

$$f(x) = \int_{\mathbb{R}^k} e^{i\hat{x}\cdot\hat{\xi}} b(\bar{x}, \hat{\xi}) d\hat{\xi}, \quad b \in S^{\mu+\frac{3}{4}-\frac{k}{2}}(\mathbb{R}^3 \times \mathbb{R}^k).$$

By partition of unity, we can assume that f is compactly supported. For $R \in \Psi^s(\mathbb{R}^3)$ properly supported, we can write

$$Rf(x) = \frac{1}{(2\pi)^3} \int_{\mathbb{R}^3} e^{i(x-y)\cdot\xi} a(x, \xi) f(y) d\xi dy, \quad a \in S^s(\mathbb{R}^3 \times \mathbb{R}^3 \times \mathbb{R}^3 \backslash 0).$$

Now we have

$$Rf(x) = \frac{1}{(2\pi)^3} \int_{\mathbb{R}^3} \int_{\mathbb{R}^3} \int_{\mathbb{R}^k} e^{i(x-y)\cdot\xi} a(x, \xi) e^{i\hat{y}\cdot\hat{\eta}} b(\bar{y}, \hat{\eta}) d\hat{\eta} d\xi dy = \frac{1}{(2\pi)^3} \int_{\mathbb{R}^k} e^{i\hat{x}\cdot\hat{\xi}} c(x, \hat{\xi}) d\hat{\xi},$$

where

$$c(x, \hat{\xi}) = \int_{\mathbb{R}^3} \int_{\mathbb{R}^{3-k}} \int_{\mathbb{R}^k} e^{i(\bar{x}-\bar{y})\cdot\bar{\xi}} a(x, \xi) e^{i\hat{y}\cdot(\hat{\eta}-\hat{\xi})} b(\bar{y}, \hat{\eta}) d\hat{\eta} d\bar{\xi} dy.$$

We let $\hat{\xi} = \lambda\hat{\theta}$ with $\lambda = |\hat{\xi}|$ and let $\hat{\alpha} = \lambda^{-1}(\hat{\eta} - \hat{\xi})$ i.e. $\hat{\eta} = \lambda\hat{\alpha} + \hat{\xi}$. Also, we let $\bar{\beta} = \lambda^{-1}\bar{\xi}$. So $\xi = (\bar{\xi}, \hat{\xi}) = \lambda(\bar{\beta}, \hat{\theta})$. After these changes of variables, we get

$$\begin{aligned} c(x, \hat{\xi}) &= \int_{\mathbb{R}^3} \int_{\mathbb{R}^{3-k}} \int_{\mathbb{R}^k} e^{i\lambda(\bar{x}-\bar{y})\cdot\bar{\beta}} a(x, (\lambda\bar{\beta}, \hat{\xi})) e^{i\lambda\hat{y}\cdot\hat{\alpha}} b(\bar{y}, \lambda\hat{\alpha} + \hat{\xi}) \lambda^3 d\hat{\alpha} d\bar{\beta} dy \\ &= (-1)^k \int_{\mathbb{R}^3} \int_{\mathbb{R}^{3-k}} \int_{\mathbb{R}^k} e^{-i\lambda[\bar{y}\cdot\bar{\beta}+\hat{y}\cdot\hat{\alpha}]} a(x, (\lambda\bar{\beta}, \hat{\xi})) b(\bar{y} + \bar{x}, \lambda\hat{\alpha} + \hat{\xi}) \lambda^3 d\hat{\alpha} d\bar{\beta} dy. \end{aligned}$$

Now we can apply stationary phase on variables $y, \hat{\alpha}, \bar{\beta}$ to obtain

$$c(x, \hat{\xi}) = C a(x, (0, \hat{\xi})) b(\bar{x}, \hat{\xi}) + \cdots,$$

which belongs to $S^{\mu+s+\frac{3}{4}-\frac{k}{2}}(\mathbb{R}^3 \times \mathbb{R}^k)$. Here C is a constant and the terms in $\cdots$ belong to $S^{\mu+s+\frac{3}{4}-\frac{k}{2}-1}(\mathbb{R}^3 \times \mathbb{R}^k)$, see for example the proof of [8, Theorem 3.4]. Thus $Rf \in I^{\mu+s}(Y)$.

(2) We know that $Rf \in I^{\mu+s}(Y)$ from part (1). We can apply Prop. 2.1 of [7] to get $K \circ Rf \in I^{p+\mu+s,l}(N^*Y, \Lambda_Y)$.

(3) We first apply Prop. 2.1 of [7] to conclude that $Kf \in I^{p+\mu,l}(N^*Y, \Lambda_Y)$. Then we know that $Kf \in I^{p+\mu+l}(N^*Y \backslash \Lambda_Y)$ and $Kf \in I^{p+\mu}(\Lambda_Y \backslash N^*Y)$ as Lagrangian distributions. For $R \in \Psi^s(\mathbb{R}^3)$, we know (see e.g. Lemma 7.2 of [8]) that $\mathrm{WF}(Ru) \subset \mathrm{WF}(u)$. Now we can apply part (1) to conclude that $R \circ Kf \in I^{p+\mu+s+l}(N^*Y \backslash \Lambda_Y)$. If the principal symbol of R vanishes on Λ_Y, we examine the proof of part (1) that the order of $R \circ Kf$ is $p + \mu - 1 + s$. This finishes the proof. □

Now let's consider using part (2) of Lemma 3.1 to reduce streaking artifacts. We take $R \in \Psi^{-s}(\mathbb{R}^3)$ with $s > 0$, for example,

$$Ru(x) = \frac{1}{(2\pi)^3} \int_{\mathbb{R}^3} e^{ix\cdot\xi}(1 - f(|\xi|/\epsilon))|\xi|^{-s}\hat{u}(\xi)d\xi$$

with f the cut-off function defined at the beginning of this section. Then we replace χ_2 by

$$\tilde{\chi}_2 = Q \circ R \circ B_\epsilon(-\Delta\psi),$$

and consider an approximation $\tilde{\chi} = \chi_1 + \tilde{\chi}_2$ of χ. Under the assumption of Lemma 3.1, if $\psi \in I^\mu(N^*Y)$, we know that $\tilde{\chi}_2 \in I^{-\frac{3}{2}-s+2+\mu,-\frac{1}{2}}(N^*Y, \Lambda_Y)$. In particular, $\tilde{\chi}$ is a Lagrangian distribution on N^*Y of order $\mu - s$ and a Lagrangian distribution of order $\mu + \frac{1}{2} - s$ on Λ_Y. Recall that the streaking artifacts are contained in Λ_Y, we conclude that by applying R, the singularities of streaking artifacts are reduced. However, this will also reduce the singularities on N^*Y.

Next we consider using part (3) of Lemma 3.1 to relatively reduce the streaking artifacts. Let $R \in \Psi^s(\mathbb{R}^3), s > 0$ with symbol vanishing on Λ_Y. For example, we can take $R = P(\partial)$ and replace χ_2 by

$$\hat{\chi}_2(x) = P(\partial) \circ Q \circ B_\epsilon(-\Delta\psi) = \frac{1}{(2\pi)^3} \int_{\mathbb{R}^3} e^{ix\xi} b_\epsilon(x, \xi)|\xi|^2\hat{\psi}(\xi)d\xi.$$

The key point is that the order of $\hat{\chi}_2 \in I^{-2+\mu+s}(N^*Y \backslash \Lambda_Y)$ is increased by $s = 2$ ($s > 0$), while the singularities $\hat{\chi}_2 \in I^{-\frac{3}{2}+\mu+s-1}(\Lambda_Y \backslash N^*Y)$ is only increased by $s - 1 = 1$. In other words, although the streaking artifacts are not reduced, the desired singularities in χ are enhanced. So the streaking artifacts are relatively reduced. As another example, we decompose the symbol

$$p(\xi) = -\frac{1}{3}(\sqrt{2}\xi_3 - \sqrt{\xi_1^2 + \xi_2^2})(\sqrt{2}\xi_3 + \sqrt{\xi_1^2 + \xi_2^2}).$$

Let $h(t)$ be a smooth cut-off function with $h(t) = 0, t < 0$. We let

(3.3)
$$Ru(x) = \frac{1}{(2\pi)^3} \int_{\mathbb{R}^3} \int_{\mathbb{R}^3} e^{i(x-y)\xi}[h(\xi_3)(\sqrt{2}\xi_3 - \sqrt{\xi_1^2 + \xi_2^2}) + h(-\xi_3)(\sqrt{2}\xi_3 + \sqrt{\xi_1^2 + \xi_2^2})]u(y)dyd\xi.$$

In particular, $R \in \Psi^1(\mathbb{R}^3)$ and the symbol of R vanish on Λ_Y.

Finally, we can combine the above two approaches. Let $\psi \in I^\mu(Y)$. For m a positive integer, we let $R \in \Psi^{-m}(\mathbb{R}^3)$ and $T \in \Psi^1(\mathbb{R}^3)$ so that the symbol of T vanishes on Λ_Y. Now we consider

$$\chi_2^\# = T^m \circ Q \circ R \circ B_\epsilon(-\Delta\psi)$$

as a substitute for χ_2. Then we have $\chi_2^\# \in I^\mu(N^*Y \backslash \Lambda_Y)$ while $\chi_2^\# \in I^{\mu-m+\frac{1}{2}}(\Lambda_Y \backslash N^*Y)$. So the streaking artifacts are reduced while the singularities on N^*Y remain of the same strength.

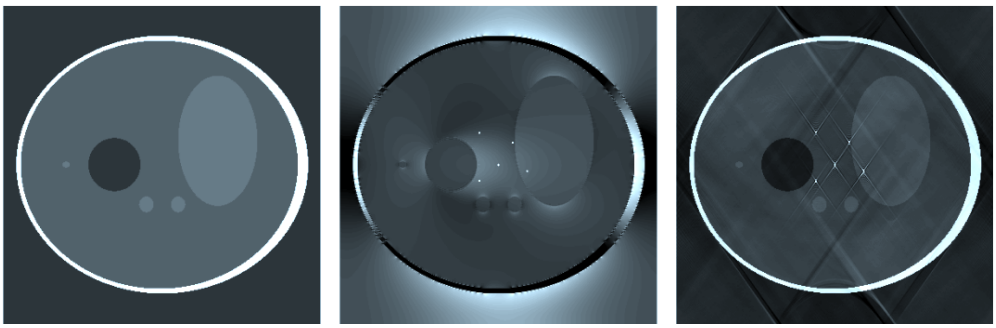

(a) (b) (c)

FIGURE 1. (a) Reference magnetic susceptibility distribution χ. (b) Simulated data ψ perturbed with point singularities. (c) Reconstructed χ using formula 2.18 in [1]. The zero cone Σ produces the propagation of singularities in the directions lying in the singular support of the fundamental solution $g(x)$ in (2.3).

4. Numerical experiments

We carried out some numerical experiments using a grid of 392x392x392 with the purpose of illustrating the above theoretical analysis on the reduction of streaking artifacts. The synthetic data was generated from the three dimensional magnetic susceptibility distribution given by the Shape-Loggan phantom following (1.2). As in [1] we perturbed the data by adding some point singularities in order to study their propagation and aiming to reduce the streaking artifacts caused by them (see figure 1). In what follows all the images correspond to sagittal views of three dimensional functions at $y = 0$, and all the images corresponding to the magnetic susceptibility distribution are displayed using a window level of [-0.3, 1]. For the data ψ we used the window level [-0.1,0.25].

One widely used reconstruction method in quantitative susceptibility mapping is the TKD method (see [1] and references therein), which aims to recover χ by direct computations following the formula

$$\hat{\chi}_\hbar(\xi) = \begin{cases} \frac{\hat{\psi}(\xi)}{D(\xi)} & \text{if } |D(\xi)| \geq \hbar, \\ \text{sign}(D(\xi))\frac{\hat{\psi}(\xi)}{\hbar} & \text{if } |D(\xi)| < \hbar. \end{cases}$$

For our experiments we implemmented a modification of the TKD method where the only difference is that we considered a smooth cut-off function to smoothly divide the Fourier Transform of the reconstructed image into two pieces, the one supported away from the characteristic set Σ and the other one supported in a neighborhood of it. Namely, the reconstructed image is of the form $\chi^\hbar = \chi_1^\hbar + \chi_2^\hbar$ with

$$\chi_1^\hbar = Q \circ (\text{Id} - B_\hbar)(-\Delta\psi), \quad \chi_2^\hbar = P_\hbar \circ Q \circ R \circ B_\hbar(-\Delta\psi), \tag{4.1}$$

where Q and $B_\hbar$ are as above respectively in (2.4) and (3.1) (with $g = 1$); $P_\hbar \in \Psi^2(\mathbb{R}^3)$ given by the symbol $\sigma(P_\hbar) = \hbar^{-1}\text{sign}(p(\xi))p(\xi)$ which vanishes in Λ_Y, and $R \in \Psi^{-2}(\mathbb{R}^3)$ given by $\sigma(R) = |\xi|^{-2}$. In the Fourier domain the previous translates into the simpler formulas

$$\hat{\chi}_1^\hbar(\xi) = (1 - b_\hbar(\xi))\frac{\hat{\psi}(\xi)}{D(\xi)}, \quad \hat{\chi}_2^\hbar(\xi) = b_\hbar(\xi)\text{sign}(p(\xi))\frac{\hat{\psi}(\xi)}{\hbar}.$$

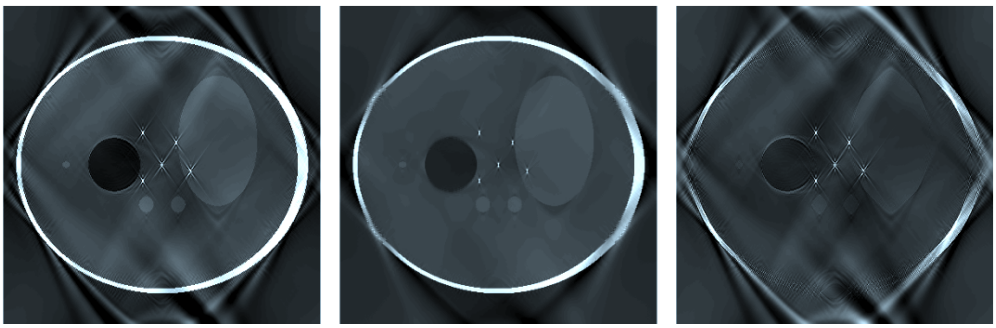

(a) (b) (c)

FIGURE 2. (a) Reconstructed susceptibility using the smooth version of the TKD method with $\hbar = 0.04$. (b) Reconstructed image using only frequencies away from the zero cone, i.e. $\chi_1^\hbar$. (c) Image obtained only considering frequencies near the zero cone, i.e. $\chi_2^\hbar$.

(a) (b) (c)

FIGURE 3. (a) Zero cone Σ. (b) Symbol of the cut-off pseudo-differential operator $B_\hbar$. (c) Symbol of the second cut-off operator $C_{M,\epsilon}$.

According to the theoretical analysis of the previous sections, what the TKD procedure does is first regularize all the singularities in directions near the zero cone by an order 2 and then enhance them, applying the operator $P_\hbar$, by and order of 2 in $N^*Y \backslash \Lambda_Y$ and 1 in $\Lambda_Y \backslash N^*Y$. Consequently, if the data belongs to $I^\mu(N^*Y)$ the streaking artifacts have order $\mu - 1/2$ and the other singularities have order μ. As one can see in figure 2(a), the streaking artifacts are slightly attenuated in contrast to figure 1(c) which was obtained by applying formula 2.18 in [1]. The artifacts are still fairly visible though making necessary to use further methods to diminish them. As mentioned above, since the streaking artifacts are caused by the zero cone Σ (figure 3(a)), removing the part of the image associated with such frequencies, this is only considering $\chi_1^\hbar$, implies lost of information as one can see in figure 2(b) where some of the edges were smoothed out. The singularities appearing in $\chi_1^\hbar$ and $\chi_2^\hbar$ are sensitive to the shape of the symbol $b_\hbar$. Indeed, if we narrow the support of the symbol it causes the presence of streaking artifacts in $\chi_1^\hbar$. A sagittal view of the function $b_\hbar$ considered in our experiments is given in figure 3(b).

We can further reduce the order of the singularities as shown in figure 4 by increasing the order of the operator R. More precisely, we consider

$$R \in \Psi^{-s}(\mathbb{R}^3) \text{ with } s > 2 \text{ and symbol } r(\xi) = K|\xi|^{-s},\ K > 0. \tag{4.2}$$

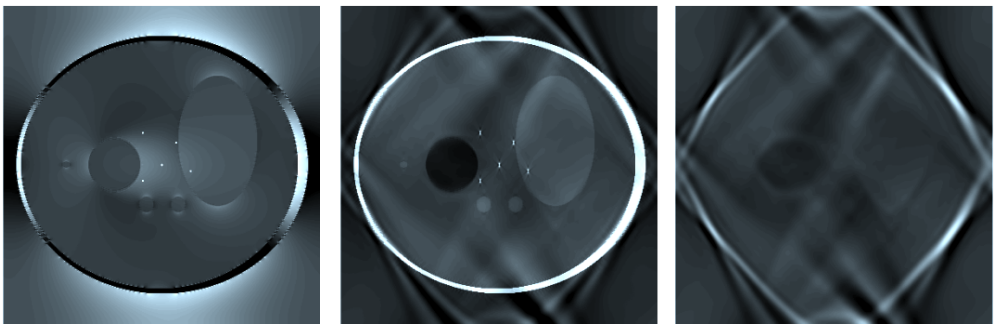

(a) (b) (c)

FIGURE 4. (a) Simulated data ψ. (b) Reconstructed image $\chi^\hbar$ applying the operator R in (4.2) with $s = 2$ and $\hbar = 0.04$. (c) $\chi_2^\hbar$. The reduction of the streaking artifacts is clear and there is less lost of information in contrast to the case of just considering $\chi_1^\hbar$ (see figure 2(b)). In (c) it can be seen that most of the smooth features contained in $\chi_2^\hbar$ are still there since R only acts on $\chi_{2,1}^\hbar$.

Moreover, for some smooth function $f \in C_0^\infty(\mathbb{R})$ such that $f(t) = 1$, $|t| < 1$ and $f(t) = 0$, $|t| > M$ for some $M > 0$, we compute $\chi_2^\hbar = \chi_{2,1}^\hbar + \chi_{2,2}^\hbar$, where

$$\chi_{2,1}^\hbar = P_\hbar \circ Q \circ R \circ (I - C) \circ B_\hbar(-\Delta\psi), \quad \chi_{2,2}^\hbar = P_\hbar \circ Q \circ C \circ B_\hbar(-\Delta\psi) \tag{4.3}$$

with $C = C_{M,\epsilon} \in \Psi^0(\mathbb{R}^3)$ of symbol $c_{M,\epsilon}(\xi) = f(|\xi|/\epsilon)$ for some $\epsilon > 0$ and $M > 0$ (see figure 3(c)). The motivation behind the division of $\chi_2^\hbar$ into two parts is that we would like to keep the smooth attributes of the image which are contained in $\chi_{2,2}^\hbar$, as well as reduce the artifacts included in $\chi_{2,1}^\hbar$. The images in figure 4 were obtained with $s = 4$, therefore the streaking artifacts are reduced to order $\mu - 1/2 - 2$ while the other singularities to order $\mu - 2$.

Finally, by considering the operator $T \in \Psi^1(\mathbb{R}^3)$ defined in (3.3) and $R \in \Psi^{-s}(\mathbb{R}^3)$ as in (4.2), the reconstructed susceptibility $\chi^\hbar = \chi_1^\hbar + \chi_2^\hbar$ in figure 5 is computed by doing $\chi_2^\hbar = \chi_{2,1}^\hbar + \chi_{2,2}^\hbar$, where $m + 2 = s > 0$ and

$$\chi_{2,1}^\hbar = (T^m \circ P_\hbar) \circ Q \circ R \circ (I - C) \circ B_\hbar(-\Delta\psi), \quad \chi_{2,2}^\hbar = P_\hbar \circ Q \circ C \circ B_\hbar(-\Delta\psi). \tag{4.4}$$

The streaking artifacts in $\chi_{2,1}^\hbar$ are reduced by an order of $-m-1/2$ while the rest of its singularities (the ones in $N^*Y \backslash \Lambda_Y$) remain in the same order μ when $\psi \in I^\mu(N^*Y)$. By implementing this procedure the streaking artifacts are further reduced, in comparison with applying just TKD, and there is no attenuation of the rest of the singularities as for instance can be noticed in figure 6, which shows the part of the reconstructed susceptibilities that contains the streaking artifacts, this is $\chi_2^\hbar$, for the previous three cases.

REFERENCES

[1] J. K. Choi, H. S. Park, S. Wang, Y. Wang, J. K. Seo. *Inverse Problem in Quantitative Susceptibility Mapping.* SIAM Journal on Imaging Sciences, 7(3), 1669-1689, 2014.

[2] J. J. Duistermaat. *Fourier integral operators.* Vol. 130. Springer Science & Business Media, 1996.

[3] M. de Hoop, G. Uhlmann, A. Vasy. *Diffraction from conormal singularities.* Annales Scientifiques de l'École Normale Supérieure, 4e serie, t. 48, (2015): 351-408.

[4] D. Finch, I. Lan, G. Uhlmann. *Microlocal analysis of the X-ray transform with sources on a curve.* Inside out: Inverse Problems and Applications 47 (2003): 193.

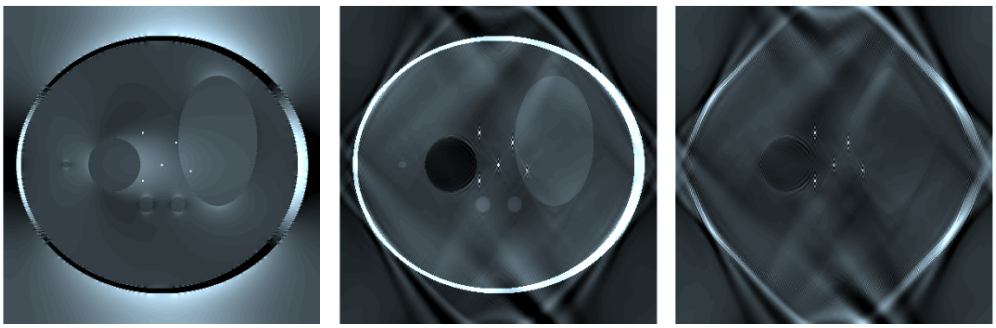

(a) (b) (c)

FIGURE 5. (a) Simulated data ψ. (b) Reconstructed susceptibility $\chi^\hbar$ following (4.4) with $m = s = 2$ and $\hbar = 0.04$. (c) $\chi_2^\hbar$. The streaking artifacts were smoothed out but not the singularities related to edges of the phantom.

(a) (b) (c)

FIGURE 6. Comparison of $\chi_2^\hbar$ in the previous three cases: (a) smooth TKD, this is following (4.1); (b) applying the operator R as in (4.3) with $s = 2$; (c) applying the operators T and R as in (4.4) with $m = 2$ and $s = 4$. Recall that the reconstructed susceptibility is given by $\chi^\hbar = \chi_1^\hbar + \chi_2^\hbar$ with the last term containing the streaking artifacts.

[5] A. Greenleaf, G. Uhlmann. *Nonlocal inversion formulas for the X-ray transform.* Duke Math. J 58.1 (1989): 205-240.

[6] A. Greenleaf, G. Uhlmann. *Estimates for singular Radon transforms and pseudodifferential operators with singular symbols.* Journal of Functional Analysis 89.1 (1990): 202-232.

[7] A. Greenleaf, G. Uhlmann. *Recovering singularities of a potential from singularities of scattering data.* Communications in Mathematical Physics 157.3 (1993): 549-572.

[8] A. Grigis, J. Sjöstrand. *Microlocal analysis for differential operators: an introduction.* Vol. 196. Cambridge University Press, 1994.

[9] V. Guillemin, G. Uhlmann. *Oscillatory integrals with singular symbols.* Duke Math. J 48.1 (1981): 251-267.

[10] L. Hörmander. *The analysis of linear differential operators I.* Grundlehren Math. Wiss 274 (1985).

[11] L. Hörmander. *The analysis of linear partial differential operators III: pseudo-differential operators.* Classics in Mathematics, 2007.

[12] L. Hörmander. *The analysis of linear partial differential operators IV: Fourier integral operators.* Classics in Mathematics, 2009.

[13] Y. Kurylev, M. Lassas, G. Uhlmann. *Seeing through spacetime.* arXiv:1405.3386 (2014).

[14] Y. Kurylev, M. Lassas, G. Uhlmann. *Inverse problems in spacetime I: Inverse problems for Einstein equations-Extended preprint version.* arXiv:1405.4503 (2014).

[15] M. Lassas, G. Uhlmann, Y. Wang. *Inverse problems for semilinear wave equations on Lorentzian manifolds.* arXiv:1606.0626 (2016).
[16] R. Melrose, G. Uhlmann. *Lagrangian intersection and the Cauchy problem.* Communications on Pure and Applied Mathematics 32.4 (1979): 483-519.
[17] J. K. Seo, E. J. Woo, U. Katscher, Y. Wang. *Electro-magnetic tissue properties MRI.* Imperial College Press, Longdon, 2014.
[18] Y. Wang. *Principles of magnetic resonance imaging: physics concepts, pulse sequences, and biomedical applications.* CreateSpace Independent Publishing Platform, 2012.

Benjamin Palacios
Department of Mathematics, University of Washington
E-mail address: bpalacio@uw.edu

Gunther Uhlmann
Department of Mathematics, University of Washington,
Institute for Advanced Study, the Hong Kong University of Science and Technology
and Department of Mathematics, University of Helsinki
E-mail address: gunther@math.washington.edu

Yiran Wang
Department of Mathematics, University of Washington,
and Institute for Advanced Study, the Hong Kong University of Science and Technology
E-mail address: wangy257@math.washington.edu